JOURNAL OF GEOPHYSICAL RESEARCH, VOL. 112, D11117, doi:10.1029/2006JD007401, 2007

An investigation into the aerosol dispersion effect through the activation process in marine stratus clouds

Yiran Peng,[1] Ulrike Lohmann,[2] Richard Leaitch,[3] and Markku Kulmala[4]

Received 13 April 2006; revised 5 December 2006; accepted 26 December 2006; published 13 June 2007.

[1] The aerosol dispersion effect (the influence of an increasing number of aerosol particles on the width of the cloud droplet size distribution) has been observed in maritime clouds [e.g., *Liu and Daum*, 2002]. Climate model simulations show that the dispersion effect at least partially compensates the first indirect aerosol effect. The application of observational data from maritime stratus/stratocumulus clouds into an adiabatic parcel model allows to analyze the role of the aerosol activation process for the dispersion effect in order to better understand the microphysical mechanism of the dispersion effect in the early stage of cloud formation. When the total aerosol number concentration is increased, the parcel model simulations show that the higher number of aerosol particles at cloud base reduces the supersaturation, which results in a slower particle growth rate, and thus more cloud droplets remain small. This extends the droplet spectra toward the smaller size end and increases the spectral width. The broadening effect partially offsets the reduction of droplet radius because of an enhanced number of aerosol particles, leading to a positive aerosol dispersion effect. Sensitivity studies show that the dispersion effect decreases for increasing updraft velocities. When the updraft velocity approaches 55 cm s^{-1}, the dispersion effect almost vanishes for maritime stratus clouds. Aerosols composed of sulfate or of less soluble organics increase the dispersion effect as compared to sea-salt aerosols, whereas condensation of gaseous nitric acid on aerosols decreases the dispersion effect in marine stratus clouds.

Citation: Peng, Y., U. Lohmann, R. Leaitch, and M. Kulmala (2007), An investigation into the aerosol dispersion effect through the activation process in marine stratus clouds, *J. Geophys. Res.*, *112*, D11117, doi:10.1029/2006JD007401.

1. Introduction

[2] One of the most uncertain factors in the current understanding of global climate forcing is the indirect aerosol effect. A rising number of aerosol particles result in an increase in the number concentration and a decrease in the size of cloud droplets. For the same cloud water content, this leads to an enhanced cloud albedo (first indirect effect [*Twomey et al.*, 1984]) and a reduced drizzle formation efficiency (second indirect effect [*Albrecht*, 1989]).

[3] To estimate the global indirect aerosol effects, aerosol-cloud interactions need to be included in global climate models (GCMs). The effective radius (r_e) of cloud droplets can be linearly related to the mean volume radius (r_v), according to observations of warm stratocumulus clouds with negligible entrainment and mixing effects [*Martin et al.*, 1994]:

$$r_e = \beta r_v \tag{1}$$

In the GCM, r_v is dependent on the predicted liquid water content and droplet number concentration (N_d) in clouds. The dispersion scaling factor β represents the influence of aerosols on the cloud droplet size distribution. Note that β is defined differently from the coefficient k used in the study by *Martin et al.* [1994]:

$$\beta = k^{-\frac{1}{3}} \tag{2}$$

[4] The first aerosol indirect effect indicates an increase of N_d and a reduction of r_e for more aerosol particles, while the aerosol dispersion effect results in a positive correlation between β and N_d (for example, observational evidence in the study by *Liu and Daum* [2002]), thus partially offsetting the first indirect effect. Including the dispersion effect in the GCM reduces the predicted global mean aerosol indirect effect [*Peng and Lohmann*, 2003, *Rotstayn and Liu*, 2003, 2005], which also partly explains the discrepancy in the

[1] Max Planck Institute for Meteorology, Hamburg, Germany.
[2] Institute for Atmospheric and Climate Science, Zurich, Switzerland.
[3] Environment Canada, Downsview, Ontario, Canada.
[4] Department of Physical Sciences, University of Helsinki, Helsinki, Finland.

0148-0227/07/2006JD007401$09.00

estimates of the indirect effect using climate model and satellite observations [*Lohmann and Lesins*, 2002]. A better understanding of the dispersion effect may improve the parameterization of aerosol-cloud interaction in a GCM and helps to reduce the uncertainties related to the aerosol indirect effect.

[5] The dispersion scaling factor (β) is an increasing function of the relative dispersion (ε) [*Liu and Daum*, 2000a, 2000b]. ε is defined as the ratio between the standard deviation (σ) and the mean radius (r_m) of the cloud droplet size distribution. Both aerosol particles and the updraft velocity at cloud base determine the cloud droplet spectral shape in the early stage of droplet formation. Entrainment and drizzle formation may further modify the droplet spectral shape at the edge or at the top of clouds. The influences of aerosol number concentration on the droplet spectral width (σ) can be very different depending on the residence time of the parcel in cloud and the height above cloud base [e.g., *Martin et al.*, 1994; *Hudson and Yum*, 2001; *Yum and Hudson*, 2001]. The present study will emphasize the effects of aerosol particles on the droplet size spectral width (σ) and the relative dispersion (ε), respectively. We investigate only the impact of the aerosol activation process on the dispersion effect.

[6] We concentrate on the role of the activation process for the dispersion effect for two reasons. First, the microphysical processes of cloud formation and precipitation development are parameterized individually in the GCM. Each process is included as a source or sink of the cloud water budget and the cloud droplet number concentration [e.g., *Lohmann et al.*, 1999]. Therefore aerosol effects on the cloud droplet number and size are treated separately for each process. Observational evidence showed that β is positively correlated with the particle number concentration in clouds when the entrainment and mixing are excluded [e.g., *Martin et al.*, 1994; *Liu and Daum*, 2002]. *Lu and Seinfeld* [2006] investigated the dispersion effect using a large-eddy simulation model, considering the collision/coalescence process, drizzle formation, and entrainment mixing. The results of *Lu and Seinfeld* [2006] indicate that the dispersion effect can be reduced or become even negative when nonadiabatic cloud processes are taken into account (note that β was used in the study by *Liu and Daum* [2002], but k was used in the works of *Martin et al.* [1994] and *Lu and Seinfeld* [2006]; cf. equation (2)).

[7] Second, the parameterization of the activation process links aerosols directly to the cloud droplet number concentration (N_d) in the GCM. Parameterizations of all subsequent processes (for example, entrainment) depend on an accurate estimation of cloud water content and the cloud droplet number concentration resulting from aerosol activation. Sophisticated activation schemes can take the vertical velocity, aerosol number, size, solubility, and chemical composition into account [e.g., *Abdul-Razzak and Ghan*, 2000]. In current GCMs, sulfate, sea salt, hygroscopic carbonaceous, and mineral dust aerosols may contribute to N_d [e.g., *Stier et al.*, 2005]. Sulfate and sea-salt aerosols are main marine aerosols. The influence of organic aerosols or volatile gases (for example, HNO_3) can be included in GCMs [*Fountoukis and Nenes*, 2005; *Romakkaniemi et al.*, 2005]. However, the contribution to the dispersion effect from the activation process remains unclear, especially how the dispersion scaling factor β depends on the aerosol chemical compositions.

[8] In the present study, a parcel model simulates the activation of aerosol particles with a uniform updraft velocity and the growth of cloud droplets by condensation of water vapor under adiabatic conditions. Processes of droplet collision/coalescence, mixing between cloudy air, and entrainment with environmental air are not taken into account; nor is the drizzle formation included. The application of aerosol and cloud measurements into the parcel model makes it possible to investigate the mechanism of the dispersion effect. Observational data from maritime clouds are used because marine stratiform clouds are an important regulator for the global radiation budget [*Hartmann et al.*, 1992].

[9] This study uses three different setups of the parcel model [*Leaitch et al.*, 1986; *Shantz et al.*, 2003; *Kulmala et al.*, 1993] in order to account for the different chemical composition of soluble aerosols. For the first setup, aerosol and cloud microphysical data taken from one case observed during the Radiation, Aerosol, and Cloud Experiment (RACE) in 1995 [*Li et al.*, 1998; *Peng et al.*, 2005] are applied to the parcel model described by *Leaitch et al.* [1986]. In this case, aerosols at cloud base are composed of sulfate and sea salt. The simulated result is analyzed to study the fundamental mechanism of the dispersion effect. The sensitivity of the dispersion effect to the updraft velocity and to changes in the chemical composition from sea salt to sulfate is also investigated for this case. For the second setup, observations from 2 days of the Canadian Surface Ocean and Lower Atmosphere Study (C-SOLAS; W. R. Leaitch et al., in preparation, 2007) are applied to the model described by *Shantz et al.* [2003] in order to investigate the impact of organic aerosols. The measurements of both RACE and C-SOLAS were made from an aircraft below, in, and above stratus or stratocumulus clouds over the Atlantic Ocean in the boreal fall (September and October). For the third setup, one cloud case with assigned size and number of aerosol particles following *Kulmala et al.* [1996] is applied to the model described by *Kulmala et al.* [1993] in order to study the effect of HNO_3 condensing on soluble aerosols. Details of the available data and applications into the parcel model are described in section 2. The methodology of analyzing the dispersion effect is addressed in section 3, simulation results are presented in section 4, and the conclusions are given in section 5.

2. Data and Model Description

[10] For the first setup, one stratus cloud observed on 8 September 1995 (Flight 18) during RACE is simulated as the standard case to analyze the dispersion effect (hereafter referred to as the STD case). The instrumentation on the aircraft in RACE is described as in the study by *Peng et al.* [2005]. The updraft velocity (w) is based on 1 standard deviation of the probability density function of the gust probe measurements (cf. Figure 2 of *Peng et al.* [2005]), indicating the degree of turbulence for this cloud case. The temperature and pressure at cloud base are 11.1°C and 985 hPa, respectively. The parcel model is initialized at a

Table 1. Properties of Aerosol Particles at Cloud Base for the STD Case: Total Number Concentration of Aerosols (N_a in cm^{-3}), Geometric Mean Radius (μm), Geometric Standard Deviation, and the Chemical Composition of Aerosols

STD	N_a	Geo. Mean Rad.	Geo. Std. Dev.	Composition
Mode 1	2740	0.05	2.00	NH_4HSO_4
Mode 2	175	0.08	1.55	NH_4HSO_4
Mode 3	9	0.8	2.00	NaCl

relative humidity of 98%. The total aerosol number concentration at cloud base and the observed peak number of cloud droplets are 2924 and 147 cm^{-3}, respectively [*Peng et al.*, 2005]. The aerosol size distribution and chemical compositions are separately given in Table 1 (cf. detailed discussion by *Peng et al.* [2005]).

[11] For the second setup, two stratocumulus clouds observed on 13 and 14 October 2003 during C-SOLAS are analyzed in order to investigate the sensitivity of the dispersion effect to less soluble organic aerosols (hereafter referred to as ORG1 case and ORG2 case). The instrumentation on the aircraft during these two flights is described by W. R. Leaitch et al., in preparation, 2007. The updraft velocity, temperature, pressure, relative humidity, aerosol number concentration at cloud base, and the peak cloud droplet number are listed in Table 2. The aerosol size distribution and chemical compositions are given in Table 3. Particles in the two accumulation modes are assumed to be an internal mixture of H_2SO_4 with a generic organic having a solubility of 5 kg m^{-3} and a molecular weight of 0.15 kg mol^{-1}. Note that the organic aerosol concentration is higher and w is larger in the ORG2 case compared with the ORG1 case.

[12] For the third setup, an artificially assigned set of data (representing for a maritime cloud; cf. *Kulmala et al.* [1996]) is used to study the influence of HNO_3 on the dispersion effect (hereafter referred to as the HNO_3 case). Initial temperature, pressure, relative humidity, updraft velocity, aerosol, and cloud droplet number concentrations are given in Table 2. Aerosols at cloud base are a mixture of ammonium sulfate and an insoluble material (the model is not sensitive to the density of the insoluble material). Both more and less hygroscopic aerosols are considered in the Aitken and the accumulation modes according to a discussion by *Kulmala et al.* [1996]. Number, size, and soluble fraction of aerosols are listed in Table 4.

Table 2. Observed Values of the Updraft Velocity (w in cm s^{-1}), Temperature (T in °C), Pressure (p in hPa), Relative Humidity (RH in %), and Total Aerosol Number Concentration (N_a in cm^{-3}) at Cloud Base and the Peak Cloud Droplet Number (N_d in cm^{-3}) for the STD Case From RACE and for the ORG1 and ORG2 Cases From C-SOLAS, respectively[a]

Quantity	RACE (STD)	C-SOLAS (ORG1)	C-SOLAS (ORG2)	Assigned (HNO_3)
w	26	13	48	10
T	11.1	17.2	12.5	20.0
p	985	960	960	950
RH	98	98	98	99
N_a	2924	663	1108	450
N_d	147	200–300	510–760	n/a

[a]Same data for the HNO_3 case but assigned artificially.

Table 3. Properties of Aerosol Particles at Cloud Base for the ORG1 and ORG2 Cases: Total Number Concentration of Aerosols (N_a in cm^{-3}), Geometric Mean Radius (μm), Geometric Standard Deviation, and the Chemical Composition of Aerosols

	N_a	Geo. Mean Rad.	Geo. Std. Dev.	Composition
ORG1				
Mode 1	40	0.01	1.50	H_2SO_4
Mode 2	398	0.03	1.48	H_2SO_4
Mode 3	203	0.09	1.27	15%Org + 85%H_2SO_4
Mode 4	22	0.25	1.25	15%Org + 85%H_2SO_4
ORG2				
Mode 1	92	0.015	1.40	H_2SO_4
Mode 2	490	0.04	1.32	H_2SO_4
Mode 3	495	0.1	1.47	80%Org + 20%H_2SO_4
Mode 4	24	0.34	1.20	30%Org + 70%H_2SO_4
Mode 5	7	0.59	1.50	NaCl

3. Methodology

[13] *Yum and Hudson* [2005] pointed out that the growth rate of particles is a crucial factor in analyzing the broadening of the cloud droplet spectrum:

$$r\frac{dr}{dt} = \frac{S_a - S_e}{(F_k + F_d)} \tag{3}$$

The growth rate ($\frac{dr}{dt}$) depends on the particle size (r), the ambient supersaturation (S_a), the equilibrium supersaturation over the droplet (S_e), the heat transition (F_k), and the vapor diffusivity (F_d) during the condensational growth. The number of aerosol particles and the updraft velocity at cloud base are the main factors for controlling S_a in the activation process [e.g., *Leaitch et al.*, 1996], and they can have strong impacts on the shape of the cloud droplet spectrum. S_e is determined by the size, surface property, soluble mass fraction, and chemical composition of aerosol particles at cloud base. The heat and water vapor transfer (F_k and F_d) during the diffusional condensation are dependent on the environmental temperature, pressure, condensation coefficient, and thermal accommodation coefficient [*Pruppacher and Klett*, 1997]. The two coefficients can be changed if the volatile gaseous aerosol (for example, HNO_3) contributes solute to particles. Therefore chemical composition of aerosols may modify S_e and $\frac{1}{F_k+F_d}$ and hence influence the droplet spectral shape as well.

[14] In the present study, parcel model simulation results are analyzed to show how more aerosol particles reduce S_a and lead to a larger gap in the growth rates between larger

Table 4. Properties of Aerosol Particles at Cloud Base for the HNO_3 Case: Total Number Concentration of Aerosols (N_a in cm^{-3}), Geometric Mean Radius (μm), Geometric Standard Deviation, and the Soluble Fraction of Aerosols

HNO_3	N_a	Geo. Mean Rad.	Geo. Std. Dev.	Sol. Frac.
Mode 1	150	0.03	1.35	0.5
Mode 2	150	0.03	1.35	0.05
Mode 3	75	0.1	1.60	0.5
Mode 4	75	0.1	1.60	0.05

and smaller aerosol particles (as shown in Figure 3 of this study and in Appendix A of *Yum and Hudson* [2005]). This mechanism regulates the shape of droplet spectrum, resulting in a broadening effect (higher σ) and contributing to the dispersion effect (higher ε, hence higher β). The sensitivity of the dispersion effect to the updraft velocity and the chemical composition of aerosol particles are also investigated.

[15] Four parameters are used to describe the shape of the cloud droplet spectrum: the mean radius (r_m), the standard deviation (the droplet spectral width/broadness, σ) of the cloud droplet size distribution, the relative dispersion ($\varepsilon = \frac{\sigma}{r_m}$), and the dispersion scaling factor β to calculate r_e from r_v in the GCM (β is positively correlated with ε; cf. *Liu and Daum* [2000a, 2000b]). Consider two identical cloud cases with the same below-cloud aerosol properties and the same updraft velocities. Double the aerosol number concentration (N_a) in the second case and keep the original N_a in the first case. The ratio of standard deviations in the two cases, σ_2 to σ_1, indicates the change of spectral width due to the increase in the particle number. It is a broadening effect if $\frac{\sigma_2}{\sigma_1} > 1$. Similarly if $\frac{\epsilon_2}{\epsilon_1}$ is larger than 1, a positive dispersion effect is indicated.

[16] To analyze the mechanism of the dispersion effect, the STD case (a reference case) and a cloud case with doubled N_a but otherwise identical to the STD case (hereafter referred to as the DBL case) were simulated with the parcel model. The ratio of $\frac{\sigma_{DBL}}{\sigma_{STD}}$ and $\frac{\epsilon_{DBL}}{\epsilon_{STD}}$ are presented in order to study the broadening and the dispersion effects. The respective contributions of r_m and σ to the dispersion effect are addressed. Knowing that β is positively correlated with ε, the changes in β due to doubled N_a will show the same behavior as ε. Therefore we mostly focus on the ratio of ε between the DBL case and the STD case to study the dispersion effect.

4. Results

4.1. Mechanism of the Dispersion Effect

[17] The parcel model simulation results from the STD case and the DBL case are shown in Figure 1. Vertical profiles of the supersaturation, the cloud droplet number concentration (N_d), the mean radius (r_m), the standard deviation (σ), and the relative dispersion (ε) are plotted as a function of the height above cloud base. The simulated N_d of 150 cm^{-3} is close to the observed value (147 cm^{-3}, Table 2). The dash-dotted line indicates where the supersaturation reaches its maximum (S_{max}). The parcel model simulations are terminated once a distinct gap occurs between the nonactivated and the smallest activated aerosol particles (cf. Figure 2). All particles with positive growth rates and with radii larger than 1 μm (cf. Figures 2 and 3) are regarded as cloud droplets [*Peng et al.*, 2005]. The steady state is defined as the height above cloud base where N_d, $\frac{\sigma_{DBL}}{\sigma_{STD}}$, and $\frac{\epsilon_{DBL}}{\epsilon_{STD}}$ remain almost constant (dotted lines in Figure 1). Figures 1a–1c show that more aerosols in the DBL case (dashed lines) result in a lower supersaturation and more but smaller cloud droplets. The ratio of σ_{DBL} to σ_{STD} at steady state (Figure 1d) indicates a broadening effect. An enhancement in ε of about 20% (Figure 1e) is the dispersion effect resulted from the doubled N_a at cloud base. The increase in σ and the decrease in r_m contribute roughly equally to the dispersion effect in this case (48% and 52%, respectively).

[18] To compare the dispersion effect to previous studies, the ratio of β_{DBL} to β_{STD} is calculated from ε_{DBL} and ε_{STD}, following equation (2) of *Liu and Daum* [2002]. $\frac{\beta_{DBL}}{\beta_{STD}}$ is 1.03 in this study. The data from *Martin et al.* [1994] yield a ratio of β of 1.06 when going from maritime air masses (with N_d = 180 cm^{-3}) to continental air masses (with N_d = 300 cm^{-3}). Their dispersion effect is larger because the increase in N_d is larger than in the STD-DBL pair simulation (cf. Figure 1b).

[19] The value of N_a in the STD case is relatively high (2924 cm^{-3}, see Table 2) for maritime clouds. Since *Lu and Seinfeld* [2006] indicate a positive dispersion effect for nonadiabatic clouds only if N_a is less than about 1000 cm^{-3}, the STD-DBL pair is rerun with one third of N_a at cloud base. The resulting ratios of ε and β are 1.09 and 1.02, respectively, because fewer N_a cause a higher supersaturation, which partly offsets the dispersion effect resulting from the doubled N_a. Therefore both ratios of ε and β are decreased, yet larger than 1. It shows that the dispersion effect through the activation process is evident whether N_a at cloud base in the clean case is rather high or low. However, if the collision/coalescence, mixing, entrainment, and drizzle formation processes are included, the dispersion effect tends to be suppressed when N_a is relatively high [*Lu and Seinfeld*, 2006].

[20] Figures 2 and 3 demonstrate the mechanism of the dispersion effect. In Figure 2, only some of the large accumulation mode particles achieve cloud droplet size at cloud base. At S_{max}, particles in the small accumulation mode (the middle mode) grow slower in the DBL case than the STD case (see also the middle panel of Figure 3) because of the lower supersaturation in the DBL case (Figure 1a), which is consistent with the discussion in the work of *Yum and Hudson* [2005]. At steady state, particles below 0.3 μm remain interstitial because of their small size. Some of the activated particles (with radii > 1 μm) in the DBL case are smaller than in the STD case; hence the droplet size distribution is extended to the small size end. As a result, the mean cloud droplet size in the DBL case is smaller and the spectral width is broader (Figure 1c and 1d), resulting in a positive dispersion effect (Figure 1e).

[21] In Figure 3, the growth rate (dr/dt) is plotted for particles of different size. As can be seen from equation (3), the larger the droplet, the lower the growth rate (note that the vertical scales are different for the three panels in Figure 3). One smaller and one larger particle are chosen and marked in orange and red, respectively, at cloud base for both STD and DBL cases. At S_{max}, the growth rate of the small particle in the DBL case (the orange square dot) is slower than for the other marked dots, which is mainly due to the lower supersaturation (S_a) in the DBL case than in the STD case (cf. equation (3) and Figure 1a). The slower growth of small particles in the DBL case results in a broader spectrum extended to the small size end, which is evident from the larger horizontal gap between the two colored square dots than that between the two cross dots at steady state (Figure 3).

4.2. Sensitivity of the Dispersion Effect to the Updraft Velocity

[22] In this section, the STD and the DBL cases are rerun with updraft velocities ranging from 16 to 51 cm s^{-1} (with a

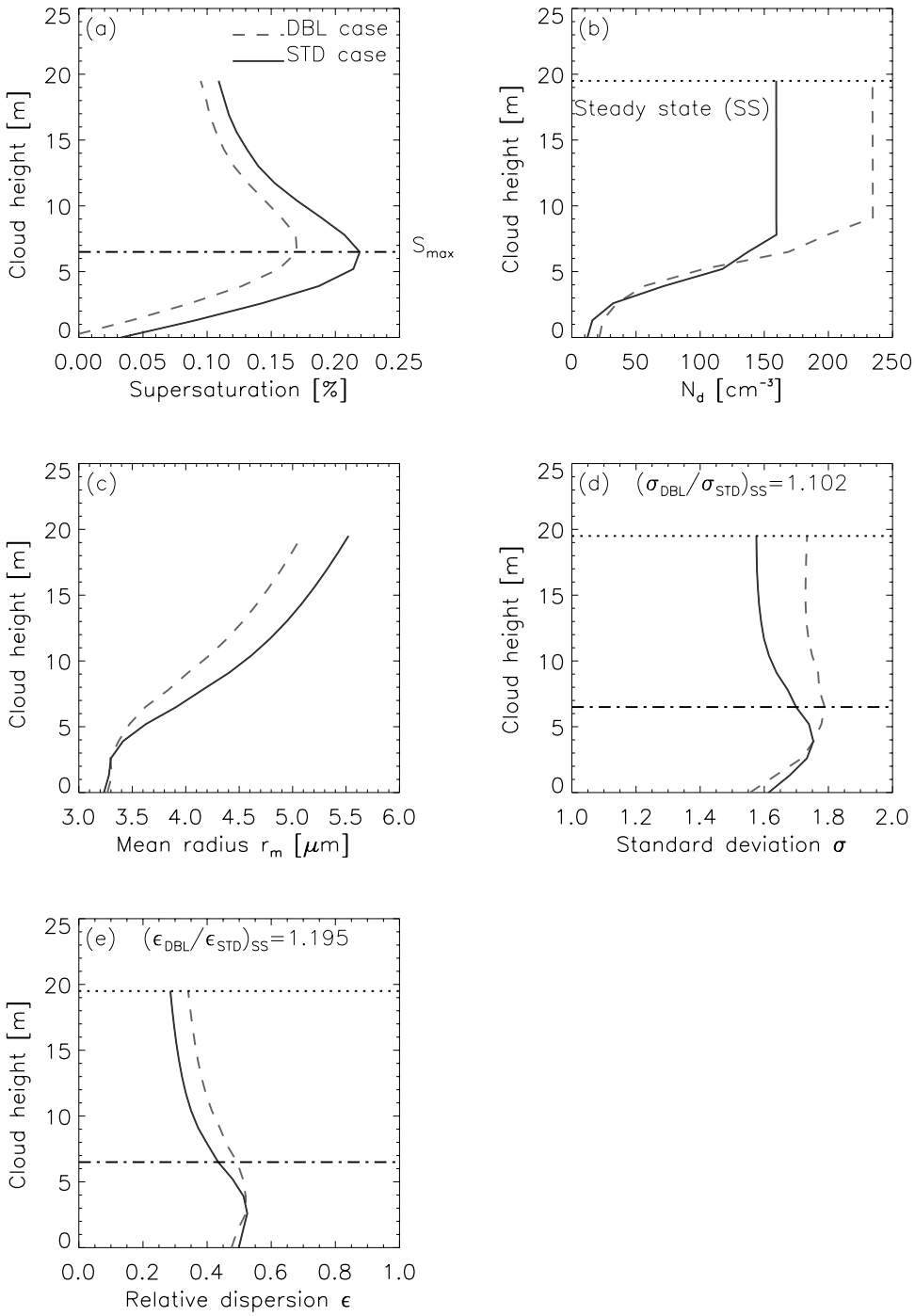

Figure 1. Comparison of cloud profiles above cloud base for the STD case and the DBL case in terms of supersaturation, cloud droplet number concentration (N_d), mean radius (r_m), standard deviation (σ), and relative dispersion (ε). S_{max} indicates the maximum supersaturation. Steady state is defined where N_d, $\frac{\sigma_{DBL}}{\sigma_{STD}}$, and $\frac{\epsilon_{DBL}}{\epsilon_{STD}}$ remain almost constant.

5 cm s^{-1} interval) in order to investigate the sensitivity of the dispersion effect to the updraft velocity.

[23] Figure 4 shows results from these simulations. Both $\frac{\sigma_{DBL}}{\sigma_{STD}}$ and $\frac{\epsilon_{DBL}}{\epsilon_{STD}}$ decrease as the updraft velocity increases, and approach 1 ($\frac{\sigma_{DBL}}{\sigma_{STD}}$ = 1.002 and $\frac{\sigma_{DBL}}{\sigma_{STD}}$ = 1.003, not shown in Figure 4) when w is 55 cm s^{-1}. The higher w increases the supersaturation (S_a in equation (3)), which counteracts the broadening of the cloud droplet spectrum resulting from the doubled N_a. Thus the dispersion effect is reduced when the updraft velocity increases and almost vanishes at w = 55 cm s^{-1}. This value is consistent with the upper bound of observed updraft velocity in marine stratus clouds [e.g., *Guibert et al.*, 2003], suggesting that the dispersion effect is more important for less turbulent clouds. However, it is worth pointing out that the updraft velocity may play a different role if other cloud processes are considered. For

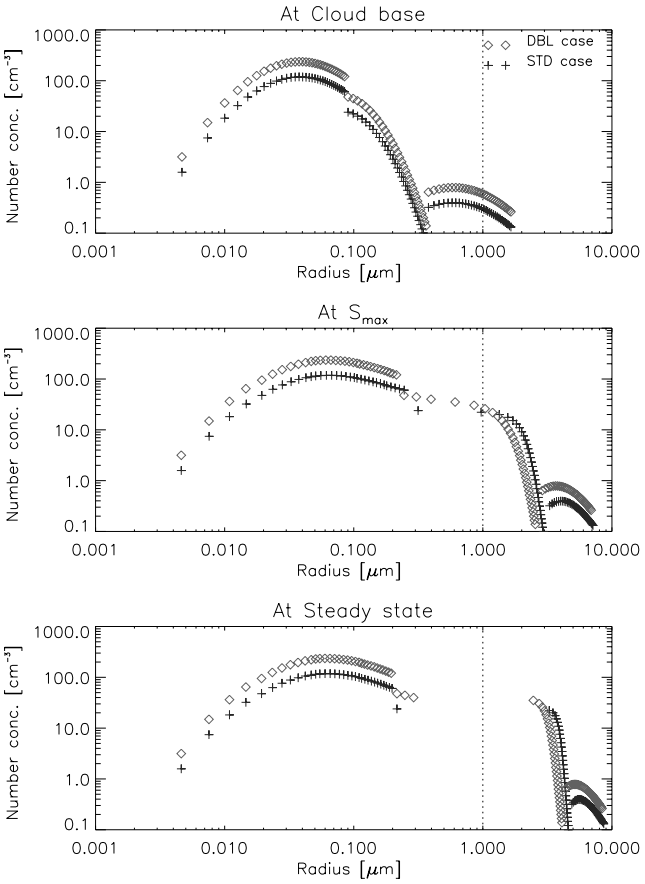

Figure 2. Comparison of the cloud droplet spectra in the STD case and in the DBL case at three stages (cf. Figure 1) of the activation process. The dotted vertical line indicates the threshold radius for cloud droplets (1 μm).

example, *Lu and Seinfeld* [2006] showed that high updraft velocity may result in an increased cloud top entrainment mixing and lead to a stronger broadening effect.

4.3. Sensitivity of the Dispersion Effect to the Aerosol Chemical Composition

[24] The aerosol composition affects the growth of cloud droplets and in turn modifies the shape of the cloud droplet size spectrum (see equation (3)). In this section, parcel model simulations are conducted for three different chemical compositions in order to investigate their influences on the dispersion effect. The impact of sulfate aerosols instead of sea-salt aerosols, less soluble organics internally mixed with sulfate aerosols, and the gaseous nitric acid condensing on sulfate aerosols are discussed in the following three subsections, respectively.

4.3.1. Effect of Sulfate Aerosols Replacing Sea-Salt Aerosols

[25] The composition of aerosols in the large accumulation mode of the STD case was assumed to be sea salt (Table 1). Sea-salt particles may be internally mixed with sulfate [*O'Dowd et al.*, 1997] when pollutants emitted from continents encounter maritime clouds [e.g., *Li et al.*, 1998]. The equilibrium supersaturation (S_e in equation (3)) required for the growth of sea-salt particles is smaller than for sulfate particles of the same size because of the lower molecular mass of sea salt [*Pruppacher and Klett*, 1997]. Thus if sea salt is replaced by sulfate in the large accumulation mode, the growth rate of sulfate particles by the water condensation will be slower compared to sea-salt particles. This reduced water uptake by sulfate particles in the large accumulation mode allows for a higher supersaturation and a faster growth of the smaller accumulation mode particles. In turn, N_d is increased [see also *Ghan et al.*, 1998] and the droplet spectrum is narrower.

[26] The STD-DBL pair simulation is rerun by altering the sea-salt aerosol in the large accumulation mode to be sulfate. Changes in the cloud droplet spectral width σ, $\frac{\sigma_{DBL}}{\sigma_{STD}}$, and $\frac{\epsilon_{DBL}}{\epsilon_{STD}}$ are summarized in Table 5. Replacing sea salt with sulfate in the large accumulation mode causes a narrowing effect (smaller σ) in both the STD and the DBL cases. This narrowing effect is less pronounced when the aerosol number concentration is higher (i.e., DBL case that has lower S_a). Thus both the broadening and the dispersion effects ($\frac{\sigma_{DBL}}{\sigma_{STD}}$ and $\frac{\epsilon_{DBL}}{\epsilon_{STD}}$) are increased when sulfate aerosols replace sea salt in the large accumulation mode (Table 5).

4.3.2. Effect of Less Soluble Organic Aerosols

[27] To investigate the sensitivity of the dispersion effect to less soluble organic aerosols, the ORG1 and ORG2 cases (Table 3) are simulated with the parcel model that has been modified to take less soluble organic species into account [*Shantz et al.*, 2003]. In these two cases, organic aerosols are observed in the accumulation mode. The ORG1 case has

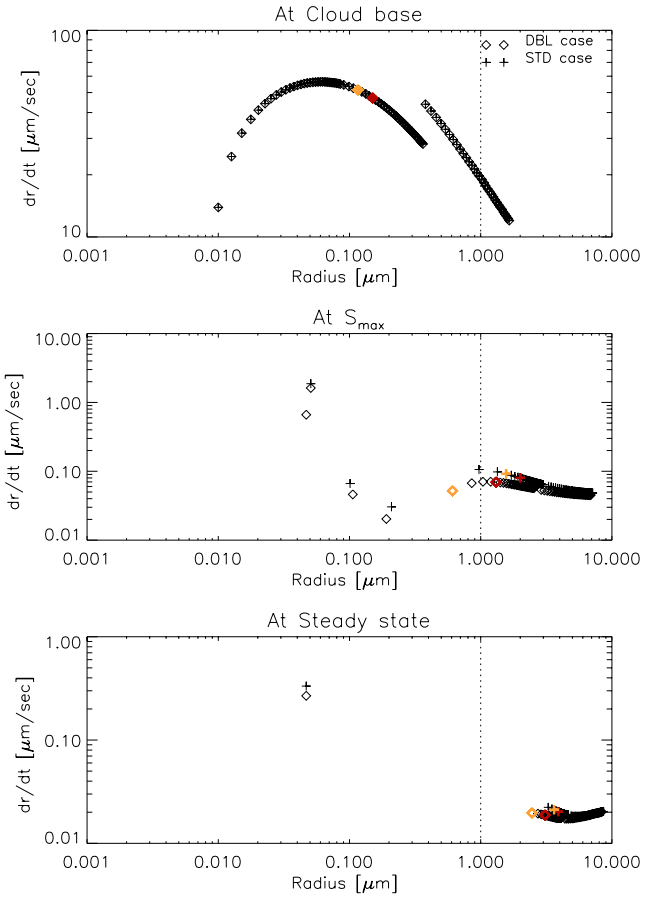

Figure 3. Same as Figure 2 but for the particle growth rate (dr/dt) in clouds.

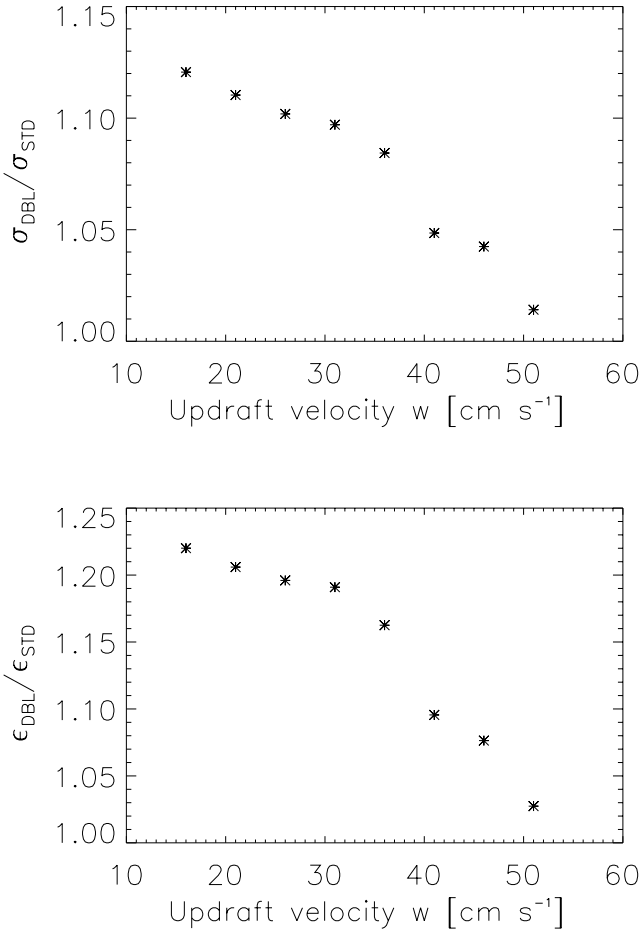

Figure 4. Sensitivity of the dispersion effect to the updraft velocity: ratios of σ_{DBL} to σ_{STD} and ε_{DBL} to ε_{STD} for different updraft velocities.

less organic mass and smaller N_a than the ORG2 case. Parcel model simulations including these generic organic aerosols obtain reasonable closure in terms of N_d (W. R. Leaitch et al., in preparation, 2007; cf. N_d in Table 2 and the two numbers of N_d marked with * in Table 6). The impact of organic aerosols in the accumulation mode strongly depends on the updraft velocity (W. R. Leaitch et al., in preparation, 2007). Thus the ORG1 and ORG2 cases are simulated with the parcel model assuming two different updraft velocities (13 and 48 cm s^{-1} in Table 2) in each case.

[28] When the updraft velocity is increased from 13 to 48 cm s^{-1}, σ is reduced (Table 6) as discussed in section 4.2. When less soluble organics are added in the accumulation mode, the influence on σ is negligible in the low organic case (ORG1), but evident in the high organic case (ORG2, cf. Table 3). Because organic aerosols are less soluble than sulfate aerosols, adding organics in the accumulation mode leads to a retarded growth of particles in the ORG2 case. Thus the cloud droplet spectrum is extended to the small size end, which results in a broadening effect (σ is increased). The broadening effect of organics is stronger when the aerosol number is higher (lower S_a further inhibits the growth of small particles, as discussed in section 4.1). As a result, both $\frac{\sigma_{DBL}}{\sigma_{STD}}$ and $\frac{\epsilon_{DBL}}{\epsilon_{STD}}$ are increased when the less soluble organic aerosols dominate the accumulation mode.

Table 5. Sensitivity of the Dispersion Effect to the Aerosol Composition in the Large Accumulation Mode: Sea Salt Versus Sulfate

Large Accu. Mode Aerosol	σ_{STD}	σ_{DBL}	$\frac{\sigma_{DBL}}{\sigma_{STD}}$	$\frac{\epsilon_{DBL}}{\epsilon_{STD}}$
Sea Salt	1.58	1.74	1.102	1.196
Sulfate	1.29	1.47	1.138	1.254

The enhancement in the dispersion effect due to the addition of organics is apparent when the updraft velocity is lower (Table 6).

[29] Replacing sea salt with sulfate and including less soluble organics result in an increased equilibrium supersaturation for aerosol particles of same size (a reduced soluble mass fraction enhances S_e in equation (3) [*Pruppacher and Klett*, 1997]). This effect on large particles in accumulation mode (section 4.3.1) or on small particles (section 4.3.2) may have completely opposite results in the droplet spectral width σ. Therefore the change in S_e has to be combined with the lower S_a resulting from the doubled N_a in order to analyze the growth rate of both large and small size particles and the dispersion effect. In this study, both sulfate and less soluble organic contaminations increase the dispersion effect.

4.3.3. Effect of Gaseous Nitric Acid

[30] Gaseous nitric acid (HNO_3) condensing on ammonium sulfate aerosols reduces the water activity of the solution droplets, which results in an increased N_d [*Kulmala et al.*, 1993] and a droplet spectral broadening [*Xue and Feingold*, 2004]. A parcel model including the semivolatile gas effect [*Kulmala et al.*, 1993] is run with the HNO_3 case (Table 4) to study the dispersion effect. *Kulmala et al.* [1995] indicated that the typical HNO_3 mixing ratio is 0.05–0.1 ppbv in maritime air and 1 ppbv in continental air. Considering possibly offshore transportation of pollutants from the land, the mixing ratios of HNO_3 are varied from 0.001 (baseline case) to 1 ppbv for the HNO_3 case. Since the influence of HNO_3 on N_d depends strongly on the mass fraction of soluble aerosols [*Korhonen et al.*, 1996], the simulation run with HNO_3 of 1 ppbv is repeated for different soluble fractions in the more and less hygroscopic modes (cf. Table 4).

Table 6. Sensitivity of the Dispersion Effect to the Aerosol Composition in the Accumulation Mode: Addition of Less Soluble Organics Versus Pure Sulfate[a]

		ORG1				ORG2			
		Organics + Sulfate		Sulfate		Organics + Sulfate		Sulfate	
w		STD	DBL	STD	DBL	STD	DBL	STD	DBL
13	N_d	*208	331	208	331	174	175	244	349
48		299	494	299	494	*503	657	496	746
13	σ	1.43	1.57	1.43	1.57	2.27	2.68	2.17	2.32
48		1.27	1.36	1.27	1.36	1.56	2.01	1.78	1.81
13	$\frac{\sigma_{DBL}}{\sigma_{STD}}$	1.10		1.10		1.11		1.09	
48		1.07		1.07		1.07		1.06	
13	$\frac{\epsilon_{DBL}}{\epsilon_{STD}}$	1.45		1.45		1.90		1.80	
48		1.33		1.33		1.64		1.58	

[a] w is in cm s^{-1} and N_d is in cm^{-3}. The number marked with * refers to results from the simulation of the observed ORG1 and ORG2 cases.

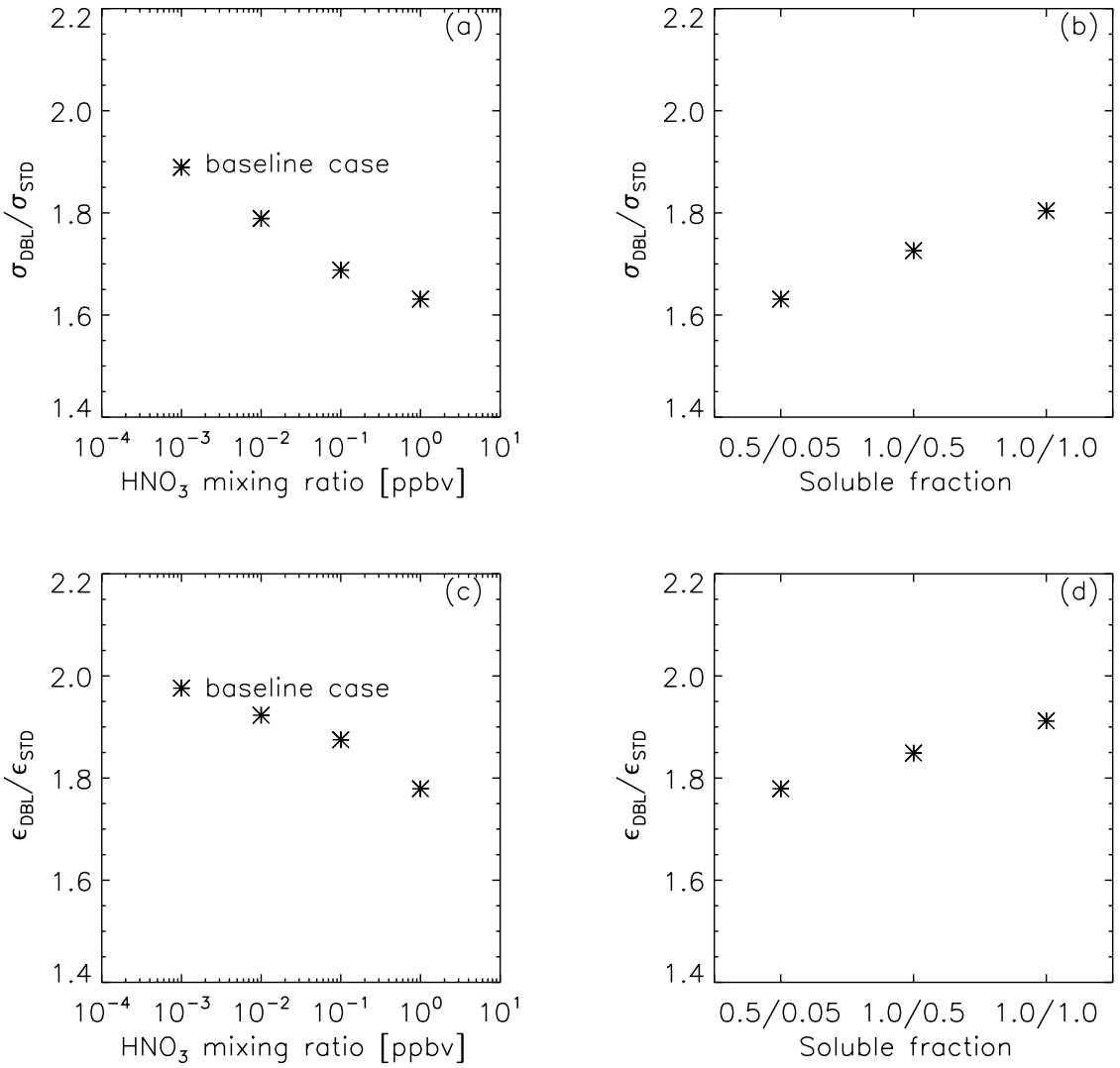

Figure 5. Sensitivity of the dispersion effect to the gaseous HNO_3: ratios of σ_{DBL} to σ_{STD} and ε_{DBL} to ε_{STD} for different HNO_3 mixing ratios (a and c) and for different soluble fractions in more and less hygroscopic modes (b and d).

[31] Ratios of σ and ε in terms of the HNO_3 mixing ratio and the soluble fraction are shown in Figure 5. The more HNO_3 that condenses on the aerosol surface, the more hygroscopic the particles become. In the parcel model, adding gaseous HNO_3 modifies the condensation coefficient and the thermal accommodation coefficient thus increasing the term $\frac{1}{F_k+F_d}$ accordingly (equation (3)). The addition of HNO_3 enhances the growth rate of particles, although the supersaturation is reduced because of the doubled N_a. As a result, the difference in the growth rate between aerosol particles of different size is decreased. Therefore both the broadening effect and the dispersion effect are damped. However, if the soluble fraction of aerosols is higher, the effect of the gaseous HNO_3 is compensated. Thus both the broadening and the dispersion effects are enhanced with an increasing soluble fraction (Figure 5).

5. Conclusions

[32] Parcel model simulations of several maritime cloud cases are studied in order to understand the mechanism of the dispersion effect in the early stage of the cloud formation process. Not only the growth rate but also the difference in the growth rate between aerosol particles of different size is a key factor that modifies the shape of the cloud droplet spectrum (Figure 3). Following equation (3), sensitivity studies show the influences of updraft velocity and aerosol chemical compositions on the dispersion effect through their modifications on S_a, S_e, and $\frac{1}{F_k+F_d}$, respectively.

[33] The results of this study will help to verify the parameterization of the activation process in GCMs. For example, a recently developed analytical expression for the relative dispersion ε [*Liu et al.*, 2006] was validated with the parcel model used in this study [*Leaitch et al.*, 1986] and showed good consistency. A positive correlation between ε and N_d, and a negative correlation between ε and w shown in the work of *Liu et al.* [2006], are similar to the results in sections 4.1 and 4.2 of this study. Additionally, the influences of organics and gaseous HNO_3 should be included in activation schemes of GCMs in order to estimate the indirect effect of anthropogenic aerosols more accurately.

The dispersion effect simulated by a GCM including these aerosol species could thus be compared to the parcel model results obtained in section 4.3 of this study.

[34] The parcel model used in the present study simulates the activation of aerosols and the diffusional growth of cloud droplets under adiabatic conditions. Thus the dispersion effect investigated here is a result only from the early stage of the cloud formation process. In addition to the activation of aerosol particles in clouds, collision/coalescence of cloud droplets leads to drizzle formation, entrainment or mixing results in an evaporation of small cloud droplets, and collection by raindrops and snowflakes reduces the number of cloud droplets. These processes add complexity to the understanding of the dispersion effect.

[35] **Acknowledgments.** The authors thank Johann Feichter, Johannes Quaas, Frank Mueller, Greg McFarquhar, and an anonymous reviewer for their constructive suggestions. Yiran Peng thanks Ilona Riipinen and Ari Asmi at Department of Physical Sciences, University of Helsinki, for their help with the cloud model including the HNO_3 effect. This research is funded by the Alexander von Humboldt Foundation in Germany.

References

Abdul-Razzak, H., and S. J. Ghan (2000), A parameterization of aerosol activation: 2. Multiple aerosol types, *J. Geophys. Res.*, *105*, 6837–6844.

Albrecht, B. (1989), Aerosols, cloud microphysics, and fractional cloudiness, *Science*, *245*, 1227–1230.

Fountoukis, C., and A. Nenes (2005), Continued development of a cloud droplet formation parameterization for global climate models, *J. Geophys. Res.*, *110*, D11212, doi:10.1029/2004JD005591.

Ghan, S. J., G. Guzman, and H. Abdul-Razzak (1998), Competition between sea salt and sulfate particles as cloud condensation nuclei, *J. Atmos. Sci.*, *55*, 3340–3347.

Guibert, S., J. R. Snider, and J.-L. Brenguier (2003), Aerosol activation in marine stratocumulus clouds: 1. Measurement validation for a closure study, *J. Geophys. Res.*, *108*(D15), 8628, doi:10.1029/2002JD002678.

Hartmann, D. L., M. E. Ockert-Bell, and M. L. Michelsen (1992), The effect of cloud type on earth's energy balance: Global analysis, *J. Clim.*, *5*, 1281–1304.

Hudson, J. G., and S. S. Yum (2001), Maritime/continental drizzle contrasts in small cumuli, *J. Atmos. Sci.*, *58*, 915–927.

Korhonen, P., M. Kulmala, H.-C. Hansson, I. B. Svenningsson, and N. Rusko (1996), Hygroscopicity of pre-existing particle distribution and formation of cloud droplets: a model study, *Atmos. Res.*, *41*, 249–266.

Kulmala, M., A. Laaksonen, P. Korhonen, T. Vesala, and T. Ahonen (1993), The effect of atmospheric nitric acid vapor on cloud condensation nucleus activation, *J. Geophys. Res.*, *98*, 22,949–22,958.

Kulmala, M., P. Korhonen, A. Laaksonen, and T. Vesala (1995), Changes in cloud properties due to NOx emissions, *Geophys. Res. Lett.*, *22*, 239–242.

Kulmala, M., P. Korhonen, T. Vesala, H. Hansson, K. Noone, and B. Svenningsson (1996), The effect of hygroscopicity on cloud droplet formation, *Tellus, Ser. B*, *48*, 347–360.

Leaitch, W. R., J. W. Strapp, and G. A. Isaac (1986), Cloud droplet nucleation and cloud scavenging of aerosol sulphate in polluted atmospheres, *Tellus, Ser. B*, *38*, 328–344.

Leaitch, W. R., et al. (1996), Physical and chemical observations in marine stratus during the 1993 North Atlantic Regional Experiment: Factors controlling cloud droplet number concentrations, *J. Geophys. Res.*, *101*, 29,123–29,136.

Li, S.-M., K. B. Strawbridge, W. R. Leaitch, and A. M. Macdonald (1998), Aerosol backscattering determined from chemical and physical properties and lidar observations over the east coast of Canada, *Geophys. Res. Lett.*, *25*, 1653–1656.

Liu, Y., and P. H. Daum (2000a), Spectral dispersion of cloud droplet size distributions and the parameterization of cloud droplet effective radius, *Geophys. Res. Lett.*, *27*, 1903–1906.

Liu, Y., and P. H. Daum (2000b), Which size distribution function to use for studies related to effective radius, *Proceedings of 13th International Conference on Clouds and Precipitation, Reno, USA*, pp. 586–589.

Liu, Y., and P. H. Daum (2002), Indirect warming effect from dispersion forcing, *Nature*, *419*, 580–581.

Liu, Y., P. H. Daum, and S. S. Yum (2006), Analytical expression for the relative dispersion of the cloud droplet size distribution, *Geophys. Res. Lett.*, *33*, L02810, doi:10.1029/2005GL024052.

Lohmann, U., and G. Lesins (2002), Stronger constraints on the anthropogenic indirect aerosol effect, *Science*, *298*, 1012–1015.

Lohmann, U., J. Feichter, C. C. Chuang, and J. E. Penner (1999), Predicting the number of cloud droplets in the ECHAM GCM, *J. Geophys. Res.*, *104*, 9169–9198.

Lu, M. L., and J. H. Seinfeld (2006), Effect of aerosol number concentration on cloud droplet dispersion: A large-eddy simulation study and implications for aerosol indirect forcing, *J. Geophys. Res.*, *111*, D02207, doi:10.1029/2005JD006419.

Martin, G. M., D. W. Johnson, and A. Spice (1994), The measurement and parameterization of effective radius of droplets in warm stratocumulus clouds, *J. Atmos. Sci.*, *51*, 1823–1842.

O'Dowd, C. D., I. E. Consterdine, and J. A. Lowe (1997), Marine aerosol, sea-salt, and the marine sulfur cycle: A short review, *Atmos. Environ.*, *31*, 73–80.

Peng, Y., and U. Lohmann (2003), Sensitivity study of spectral dispersion of the cloud droplet size distribution on the indirect aerosol effect, *Geophys. Res. Lett.*, *30*(10), 1507, doi:10.1029/2003GL017192.

Peng, Y., U. Lohmann, and R. Leaitch (2005), Importance of vertical velocity variations in the cloud nucleation process of marine stratus clouds, *J. Geophys. Res.*, *110*, D21213, doi:10.1029/2004JD004922.

Pruppacher, H. R., and J. D. Klett (1997), *Microphysics of Clouds and Precipitation*, Springer, New York.

Romakkaniemi, S., H. Kokkola, and A. Laaksonen (2005), Parameterization of the nitric acid effect on CCN activation, *Atmos. Chem. Phys.*, *5*, 879–885.

Rotstayn, L. D., and Y. Liu (2003), Sensitivity of the indirect aerosol effect to the parameterization of cloud droplet spectral dispersion, *J. Clim.*, *16*, 3476–3481.

Rotstayn, L. D., and Y. Liu (2005), A smaller global estimate of the second indirect aerosol effect, *Geophys. Res. Lett.*, *32*, L05708, doi:10.1029/2004GL021922.

Shantz, N. C., W. R. Leaitch, and P. F. Caffrey (2003), Effect of organics of low solubility on the growth rate of cloud droplets, *J. Geophys. Res.*, *108*(D5), 4168, doi:10.1029/2002JD002540.

Stier, P., et al. (2005), The aerosol-climate model ECHAM5-HAM, *Atmos. Chem. Phys.*, *5*, 1125–1156.

Twomey, S. A., M. Piepgrass, and T. L. Wolfe (1984), An assessment of the impact of pollution on global cloud albedo, *Tellus*, *36B*, 356–366.

Xue, H., and G. Feingold (2004), A modeling study of the effect of nitric acid on cloud properties, *J. Geophys. Res.*, *109*, D18204, doi:10.1029/2004JD004750.

Yum, S. S., and J. G. Hudson (2001), Microphysical relationships in warm clouds, *Atmos. Res.*, *57*, 81–104.

Yum, S. S., and J. G. Hudson (2005), Adiabatic predictions and observations of cloud droplet spectral broadness, *Atmos. Res.*, *73*, 203–223.

M. Kulmala, Department of Physical Sciences, University of Helsinki, P.O. Box 64, FIN-00014, Finland. (kulmala@cc.helsinki.fi)

R. Leaitch, Environment Canada, 4905 Dufferin Street, Downsview, Canada ON M3H 5T4. (richard.leaitch@ec.gc.ca)

U. Lohmann, Institute for Atmospheric and Climate Science, ETH Zurich, Switzerland. (ulrike.lohmann@env.ethz.ch)

Y. Peng, Max Planck Institute for Meteorology, Hamburg, Germany. (yiran.peng@zmaw.de)